Journal of Innovative Technology, Vol. 8, No. 2, pp. 119-135, September 2026
http://doi.org/10.29424/JIT.202609_8(2).0010

Numerical methods for solving nonlinear Heartbeat model of Van Der Pol oscillatory problems

Fiaz Hussain Shah [1], Muhammad Asif Zahoor Raja [2*]

ABSTRACT

The aim of the present study is to investigate numerical methods used to analyze the dynamics of the heartbeat model (HBM) represented by nonlinear coupled differential-order systems. Methods used in this study for HBMs include the Adams predictor-corrector (APC) scheme, Backward Difference Formula (BDF), adaptive explicit Runge-Kutta (AE-RK) solver, adaptive implicit Runge-Kutta (AI-RK) method, and the Livermore solver for ordinary differential equations (LSOD) procedure, along with stiffness switching extensions (SS). These numerical computing methodologies are applied to analyze the dynamics of different problems associated with HBM by variation of muscle vibration, muscle fiber tension, and fiber length. The solution of the Adam method was taken as a reference to compare with the counterpart numerical computing paradigm to verify the accuracy of each method for solving the HBMs. The absolute error was consistently in the range of 10-06 to 10-08 for each scenario of HBMs, which established the precision. Additionally, the complexity analysis was carried out for each method in terms of assessment of time of execution, number of evaluations, total number of steps, maximum error, and memory captured for all HBMs. Complexity and accuracy metrics indicated that all numerical computing schemes are in good agreement with the APC scheme, but the AE-RK is relatively better than the rest of the counterparts.

Keywords: Bioinformatics; heartbeat Model; Nonlinear system of ODEs; Numerical Methods

1. INTRODUCTION

Now a days to understand the Heart electrophysiology [1] and to design the biomedical and clinical interventions [2] the mathematical modeling of HBM [3] has become very important. The heartbeat is carried out due to the complex electrical activity [4] which is started at the cellular level and propagate across tissues of heart, which results in the synchronized contraction of the heart chambers [5]. As the experimental exploration at this scale is invasive and costly, therefor computational models [6] provide an ethically viable, reproducible and controllable platform to study the mechanisms for cardiac activity. Over time, researchers have developed a wide range of heartbeat models [7-8], from simple specific activity oscillators [9] to whole organ simulations including multi physics [10]. In these articles modelling of HBM at each level establishes different numerical challenges that motivates the researchers to develop the different numerical techniques. In the recent years, different studies have been carried out to simulate from single cell activities to multiorgan level behavior of, which enable comprehensive insight to drug responses, arrhythmia mechanisms, and planning of patient-specific therapy [11].

In the previous Heartbeat models mathematical modelling was carried out by simply nonlinear oscillators such as those inspired by the FitzHugh Nagumo [12] or van der Pol systems [13] to mimic the qualitative features of the relaxation oscillations. These modified models behaved as conceptual bridges between mathematics and physiology, which offers the computationally more efficient platforms for bifurcation analysis [14] , parameter sensitivity [16] and control studies [17]. As the demand for reliability increased, these models were modified by incorporating more variables like gating variables [18], key ion channels [19], and action-potential waveforms [20], which facilitate the detailed studies of HBM under pathological and healthy conditions. From the comprehensive study of these models highlighted thier increasing role in predictive applications [21], also the research have been carried out at the small scale like tissue/organ scale [22].

To Simulate such models researchers faced several computational and numerical challenges [23] like ionic current dynamics often exhibit stiff behaviour due to fast depolarization [24] and slow recovery phases, spatial discretization of organ-scale domains generate extremely large systems with high memory and computational demands , and multiscale temporal behavior spans microseconds to seconds or beyond. To cope with this, a variety of numerical techniques have been used like adaptive time-stepping [25], explicit/implicit time integrators [26], finite difference spatial discretization [27], operator splitting to decouple reaction and diffusion [28], and parallel algorithms and GPU acceleration [29]. The recent research on algebraic multigrid solvers have increased computation performance in HBM modelling [30]. The initiation of modified computational models of HBM presents new demands on numerical techniques and computational road map like electroanatomic mapping data, calibrating models from imaging, ver-

Manuscript received June 22, 2026; revised July 28, 2026; accepted August 30, 2026.

[1*] PhD Scholar, Graduate School of Engineering Science and Technology, National Yunlin University of Science and Technology, Taiwan R.O.C.

[2*] Professor (corresponding author), Graduate School of Engineering Science and Technology, National Yunlin University of Science and Technology, Taiwan R.O.C. (email: rajamaz@yuntech.edu.tw)

ifying and validating models under realistic conditions, achieving clinically relevant runtimes, and quantifying uncertainties [31]. In parallel, reviews prominence the trade-offs between computational tractability and model complexity, specifically for atrial modelling where structural heterogeneities such as anisotropy and fibrosis must be considered [32].

The research community has published a lot of articles in the field of HBM; according to the Web of Science database [33], the research in this field is broadly distributed across different subject categories, as given in Figure 1.

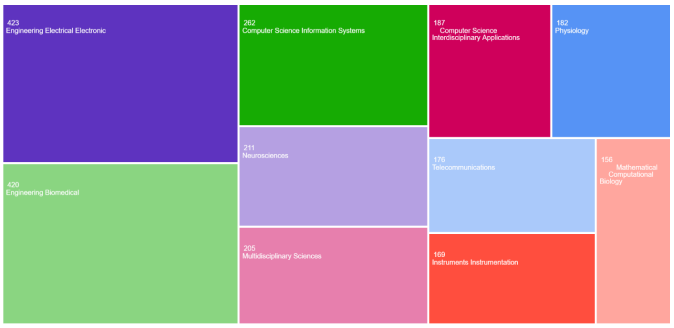


Fig. 1 web of science Subject wise database

Mostly the research is published in Electrical and Electronic Engineering and Biomedical Engineering with 423 and 420 publications respectively, which indicate that this field is mainly motivated by system modeling, biomedical instrumentation and signal processing. In addition to above areas, "Computer Science Information Systems" and "Computer Science Interdisciplinary Applications" have 262 and 187 publications respectively. The key focus in these fields are intelligent healthcare systems, and development of machine learning algorithms. Also the Neurosciences and Physiology having 211 and 182 publications respectively provide the basis for identifying the cardiac and neural collaborations. These fields mainly focus on heartbeat-induced brain responses, and regulation of autonomic system of nerves, which are very important basis for understanding physiology of heart-brain coupling.

Further related areas such as Telecommunications, Instrumentation and Sensors, and Mathematical Computational Biology have 176, 169 and 156 publications, supplementary improve the growth of HBM research by aiding remote health monitoring, mathematical modeling and designing cutting-edge biomedical device for HBM. Overall, Subject wise categorization of Web of Science in the field of HBM illustrate that this field is depicted by a strong conjunction of biomedical disciplines with computational sciences, and engineering. In Figure 2, research articles published per year for the span of 10 years from 2017 to 20126 have been given. According to this figure, the number of articles increased every year till 2023; in 2024, it decreased a little bit, but from 2025 it starts increasing, and at the end of 2026 it will cross the previous year.

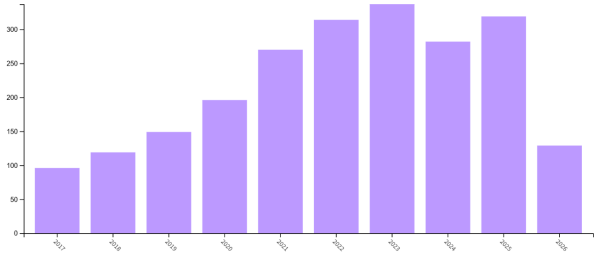


Fig. 2 web of science year wise database for last 10 years

In Figure 3, a country-wise publication database has been provided for the last 10 years in the field of HBM. Most papers were published from India (238, England (229, Germany 219, and last was Iran with 40 papers. Given the above study, our present work is based on applying and comparing different numerical techniques to the heartbeat oscillatory model, chosen for its timescale separation, relative simplicity, and combination of nonlinearity. Our goal is to evaluate each methodology in terms of efficiency, accuracy, cost, and stability, and thus to find suitable solvers for more complex HBM simulation environments. This designed comparison contributes directly to improving the numerical consistency of HBM simulations and furthermore encourages the interpretation of computational modeling into biomedical applications.

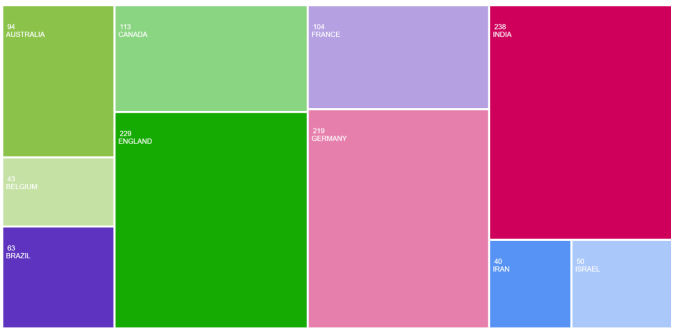


Fig. 3 web of science country wise data base for last 10 years

Salient features of the designed numerical computing paradigms are given as follows:

- Objective: The aim of the presented study is to investigate numerical methods that are used to analyze the dynamics of the heartbeat model (HBM) represented with nonlinear coupled differential-order systems.
- Methods: Methods used in this study for HBMs include the Adams predictor-corrector (APC) scheme, adaptive explicit Runge-Kutta (AE-RK) solver, adaptive implicit Runge-Kutta (AI-RK) method, and the Livermore solver for ordinary differential equations (LSOD) procedure, along with extrapolation and stiffness-switching extensions.
- Applications: These numerical computing methodologies are applied to analyzed the dynamics of different problems associated with HBM by variation of vibration of muscle, muscle fiber tension, and fiber length.
- Precision: The absolute error is consistently in the range of 10-06 to 10-08 consistently of each scenario of HBMs that the precision of AE-RK is relatively better.
- Complexity: The complexity analysis was carried out for each method in terms of assessment of time of execution, number of evaluations, total number of step counts, maximum error, and memory captured for all HBMs.

2. SYSTEM MODEL: HEARTBEAT MODEL HBM

In this study, a nonlinear control heartbeat Model is presented, which has two states, i.e., relaxed state and contracted state (systole). The heart works on these two states to pump blood throughout the body. A small electrical activity takes place inside the heart, which causes contraction in the heart muscles, resulting in pumping blood, and then it relaxes to its previous position, and blood is pumped back to the heart; therefore, by contraction and relaxation, it works as a nonlinear periodic system.

Mathematically, HBM can be presented in the equation given below [34]; it completely mimics heart functions such as the diastolic state, the systolic state, and also the threshold for the heart to go into contraction.

where χ_1 and χ_2 represents muscle fiber length and electrochemical activity of the heart; A is the smallest fast eigenvalue of the system; F and B represent the length and tension of the heart muscle fiber in the diastolic state.

$$\begin{aligned} A\dot{\chi}_1 &= -\left(\chi_1^3 - B\chi_1 + \chi_2\right) \qquad B > 0 \\ \dot{\chi}_2 &= \chi_1 - F \qquad (1) \\ \chi_1(0) &= a_1 \qquad \chi_2(0) = a_2 \end{aligned}$$

3. METHODOLOGY: NUMERICAL COMPUTING PARADIGMS

In this study of the heartbeat model, we have used different numerical techniques, i.e, the Adams predictor-corrector (APC) scheme, Backward Difference Formula, adaptive explicit Runge-Kutta, adaptive implicit Runge-Kutta method, and the Livermore solver for ordinary differential equation procedures, along with stiffness-switching extensions.

Adams: The Adams method is a widely used numerical technique for solving ordinary differential equations (ODEs). It belongs to the larger class of linear multistep methods (LMMs) and offers high accuracy with relatively low computational cost once initial steps are known.

Backward Difference Formula: The BDS method is an inherent multistep time-integration methodology used to solve stiff systems arising in fluid dynamics, chemical kinetics, and cardiac models. It uses current and previous values for approximation of the time derivative; that's why it is much more stable for stiff problems where other methods fail.

Explicit Runge–Kutta methods: Explicit Runge–Kutta methods form a widely used class of numerical integrators for solving ordinary differential equations (ODEs). They advance the solution using a sequence of intermediate stage evaluations, all computed explicitly from previously known values. This makes ERK methods easy to implement, stable for non-stiff problems, and suitable for general-purpose ODE solvers.

Implicit Runge Kutta: Implicit Runge Kutta methods form a powerful class of numerical integrators for solving stiff and non-stiff ordinary differential equations (ODEs). Unlike explicit Runge–Kutta methods, the IRK methods require solving coupled nonlinear algebraic equations at each step, but they offer superior stability, making them ideal for stiff systems commonly seen in engineering and boundary-coupled differential models such as HBD equations.

Stiffness switching: Stiffness switching is a numerical strategy used to efficiently solve differential equations that contain both stiff and non-stiff regions. It combines explicit and implicit methods within a single solver, dynamically switching between them based on the local stiffness of the system. This is particularly useful for Hybrid Boundary Differential (HBD) equations, where boundary interactions can introduce intermittent stiffness.

Livermore solver for ordinary differential equations: Livermore Solver for Ordinary Differential Equations with automatic stiffness detection. It is a widely used adaptive solver designed for efficiently integrating both stiff and non-stiff ODE systems, making it suitable for complex problems such as Hybrid Boundary Differential (HBD) equations.

4. RESULTS AND DISCUSSION

The nonlinear HBM, represented in the form of coupled ODEs, was numerically solved using Adams, BDS, Explicit Runge–Kutta (ERK), Implicit Runge–Kutta (IRK), Stiffness Switching, and LSOD methods. Here, the Adams method was used as the reference solution for all the other techniques, and the rest of the techniques were evaluated in terms of stability, accuracy, and computational efficiency. The time interval was taken over t = [0, 20] for all the simulations, which captures the transient as well as periodic steady-state behavior of the system.

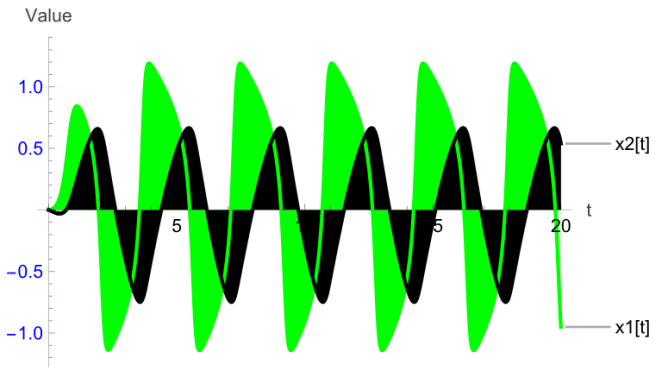
To analytically inspect the impact of our model parameters, this study was divided into three problems, and each problem has four subcases. In each Problem, we have changed the values of a specific parameter while keeping the fixed values for other parameters. Problem 1 examines the variations and effects of the fast eigenvalue factor A; Problem 2 deals with the variation in the muscle fiber tension B; and finally, in Problem 3, the variation in the diastolic muscle fiber length F is analyzed. Each figure in all problems comprises two curves representing the corresponding state variables x1 and x2. Every figure contains four graphs from a to d, representing each subcase of every problem, and each problem consists of six figures representing each methodology, i.e., APC, BDF, AE-RK, AI-RK, stiffness switching, and LSOD, respectively.

4.1 Problem 1: Effect of Electric activation rate parameter A

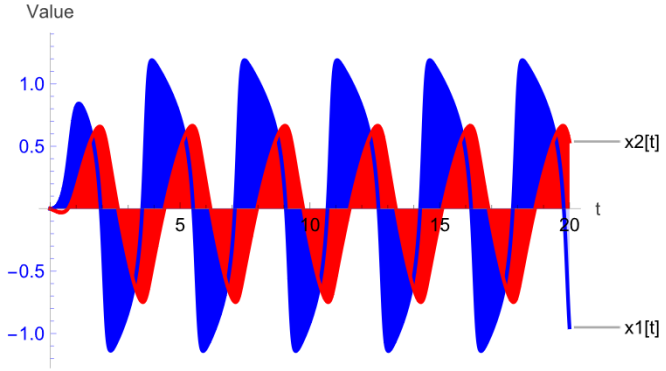
In this Problem, we have considered four different values of the fast eigenvalue A=0.2, 0.3, 0.4, and 0.5 to study HBM, while muscle fiber tension B and muscle fiber length F were taken as constant 1 and 0.1, respectively, for all four subcases. The eigenvalue parameter A is mainly responsible for the stiffness and reaction speed of HBM. The numerical results for the state variables x1 and x2 imply that higher values of A result in higher oscillations, which result in faster alterations within the fixed interval of time. The results have been shown in Figures 4 to 9; each figure represents each proposed methodology, and each figure is divided into subplots, which represent each case of Problem 1.

For the lower values of the eigenvalue parameter A, all proposed methods present an excellent response, as we have observed from subplots of every figure nearly overlapping the other figures. The results are periodic and smooth, indicating a slightly stiff system. However, when the value of A is increased, the effects of stiffness become more obvious. The AE-RK method given in figure 6 start to show phase lag and small distortion in amplitude, especially close to ultimate regions. The Adams predictor-corrector (APC method in Figure 4, used as a reference, exhibits small flattening of crisp gradients due to limitations in step size.

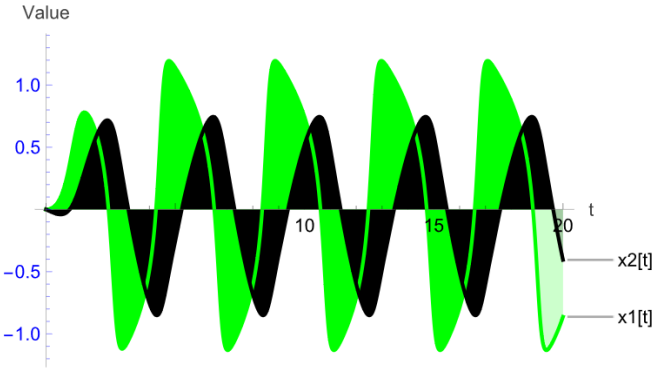
On the other hand, the explicit Runge-Kutta method in Figure 7, Stiffness Switching in Figure 5, and LSOD in Figure 6 exhibit great stability and hold close agreement with the estimated solution across all cases of Problem 1. The backward difference method given in Figure 5 also presents the exact solution but with extra computational cost. These observations verify that for higher values of the electric activation rate parameter, the system stiffness requires the use of adaptive solvers.



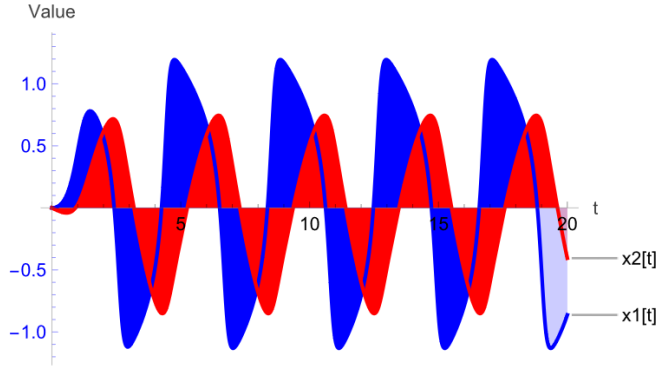
Case 1: electric activation rate parameter A=0.2



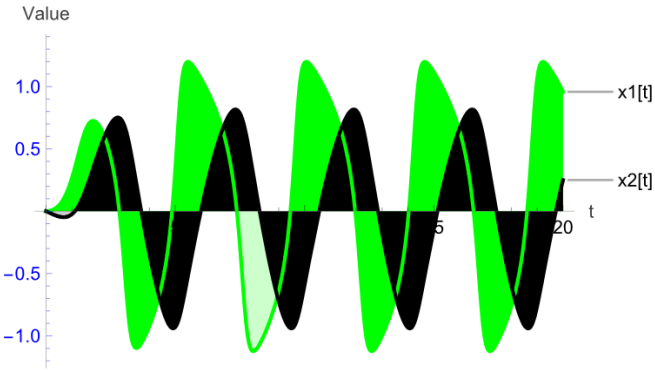
Case 1: electric activation rate parameter A=0.2



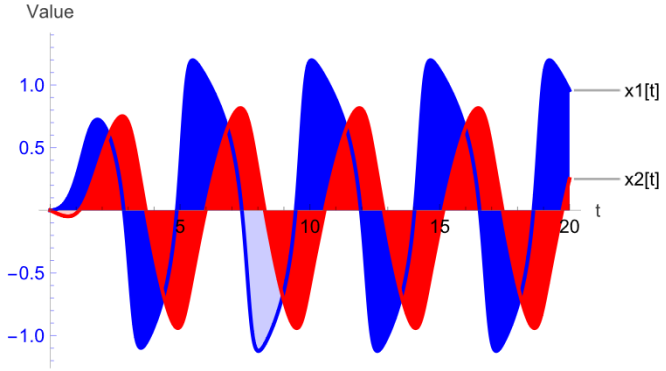
Case 2: electric activation rate parameter A=0.3



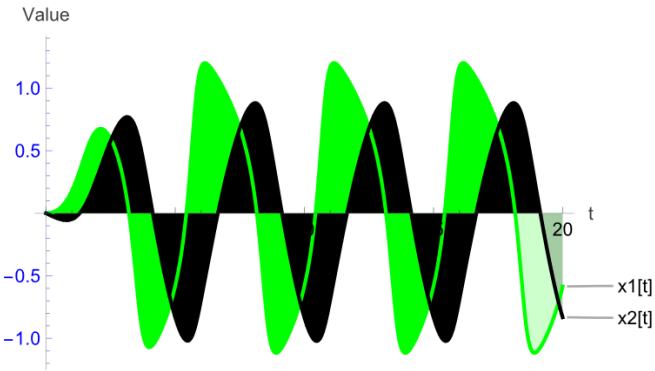
Case 2: electric activation rate parameter A=0.3



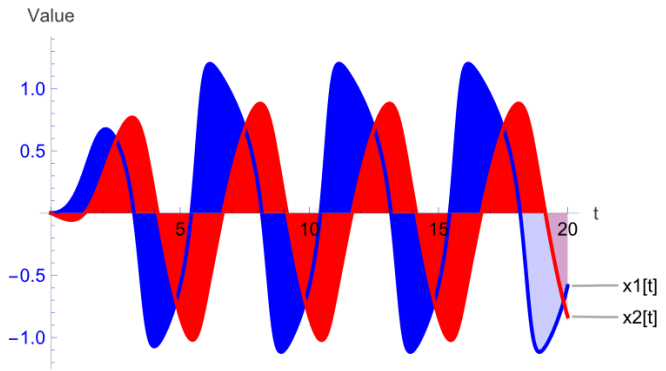
Case 3: electric activation rate parameter A=0.4



Case 3: electric activation rate parameter A=0.4



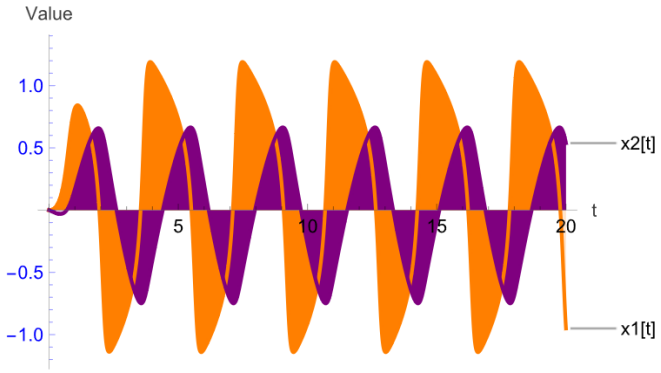
Case 4: electric activation rate parameter A=0.5



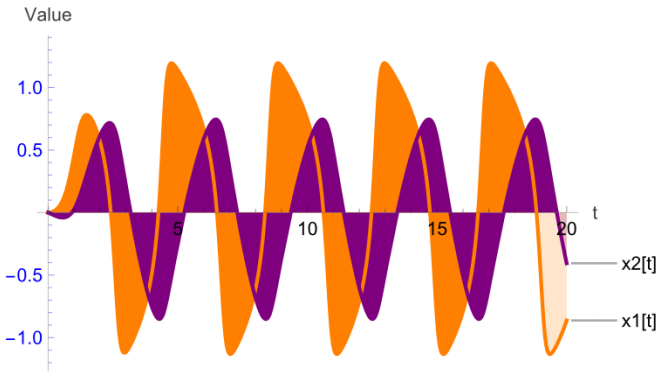
Case 4: electric activation rate parameter A=0.5

Fig. 4 Effect of variation in electric activation rate parameter on both state variables of heartbeat model by using Adams predictor-corrector (APC)

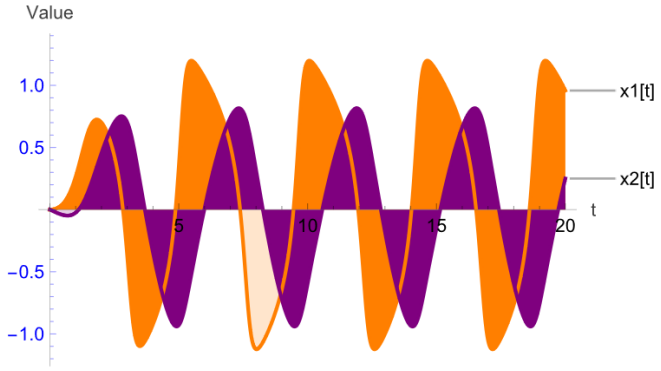
Fig. 5 Effect of variation in electric activation rate parameter on both state variables of heartbeat model by using Backward difference formula



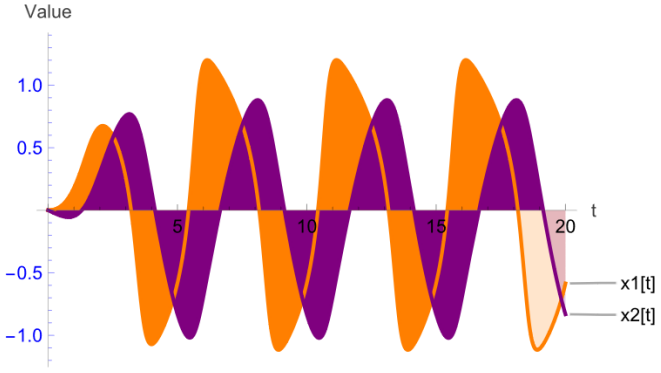
Case 1: electric activation rate parameter A=0.2



Case 2: electric activation rate parameter A=0.3

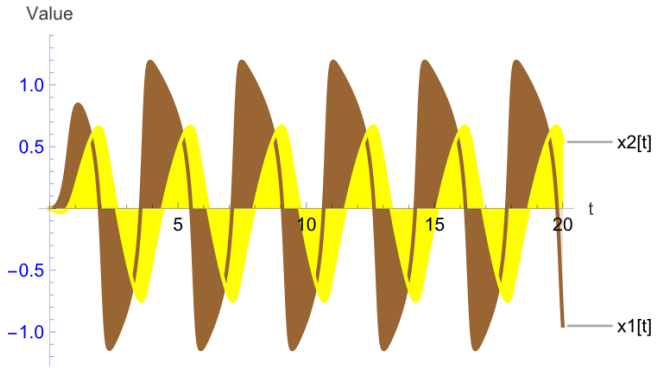


Case 3: electric activation rate parameter A=0.4

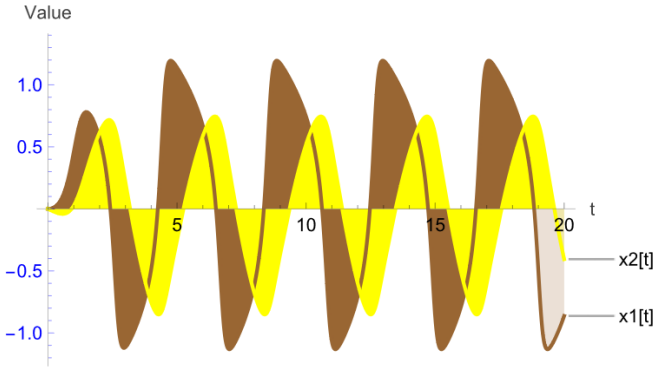


Case 4: electric activation rate parameter A=0.5

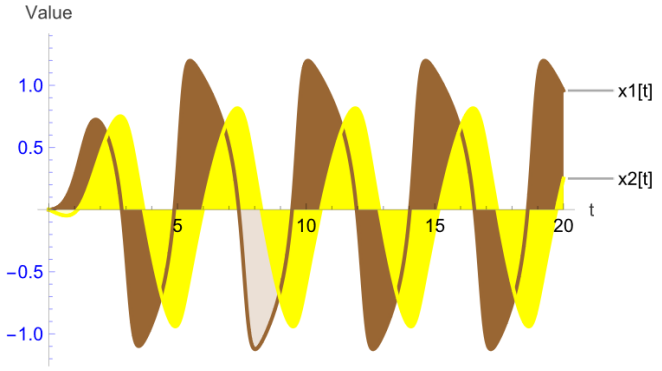
Fig. 6 Effect of variation in electric activation rate parameter on both state variables of heartbeat model by using Explicit Runge–Kutta methods



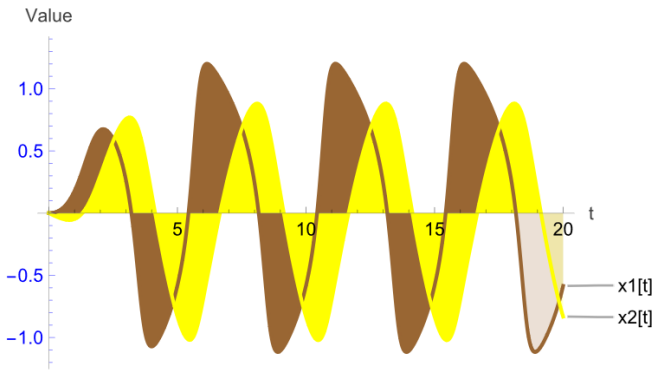
Case 1: electric activation rate parameter A=0.2



Case 2: electric activation rate parameter A=0.3

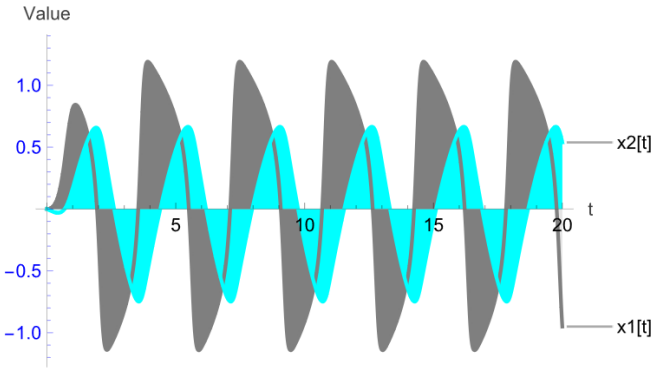


Case 3: electric activation rate parameter A=0.4

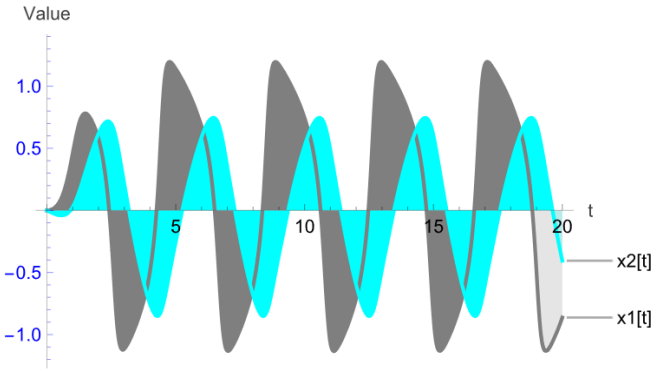


Case 4: electric activation rate parameter A=0.5

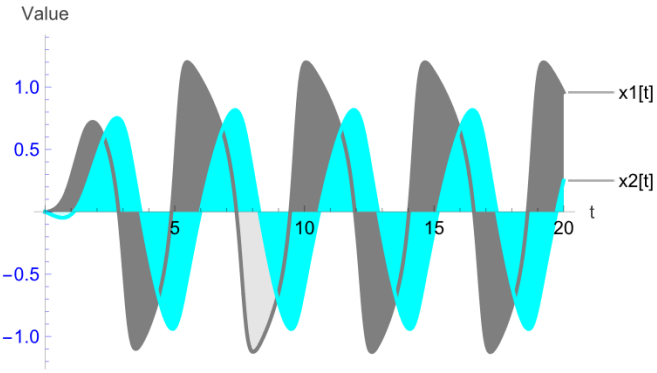
Fig. 7 Effect of variation in electric activation rate parameter on both state variables of heartbeat model by using Implicit Runge Kutta method



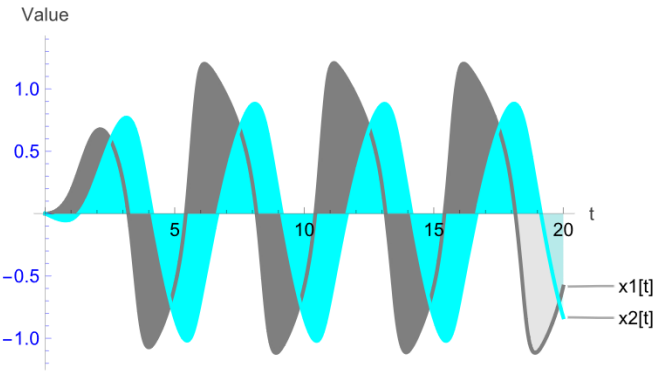
Case 1: electric activation rate parameter A=0.2



Case 2: electric activation rate parameter A=0.3

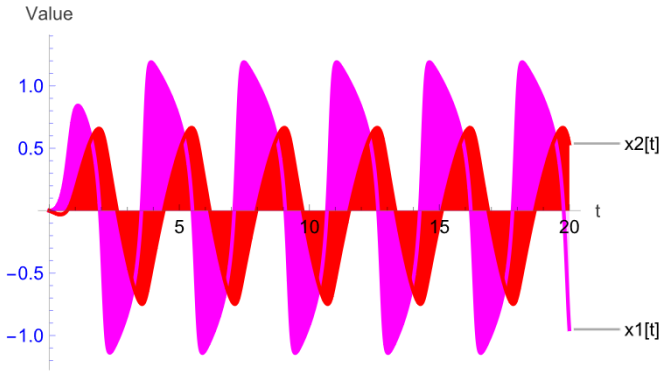


Case 3: electric activation rate parameter A=0.4

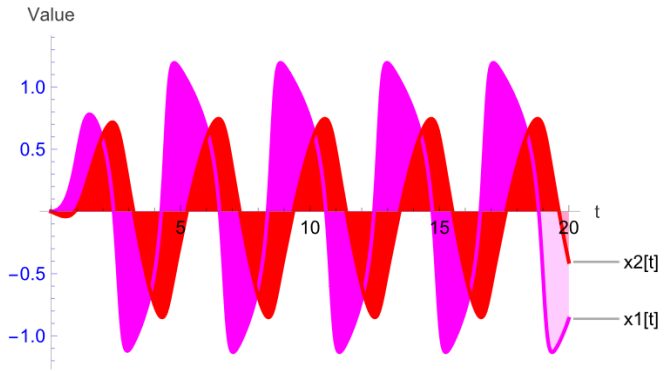


Case 4: electric activation rate parameter A=0.5

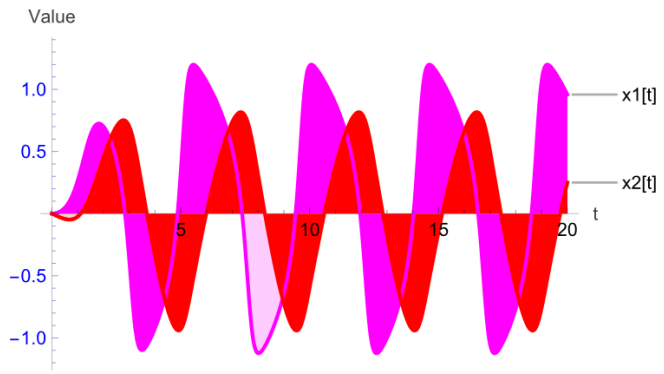
Fig. 8 Effect of variation in electric activation rate parameter on both state variables of heartbeat model by using Stiffness switching method



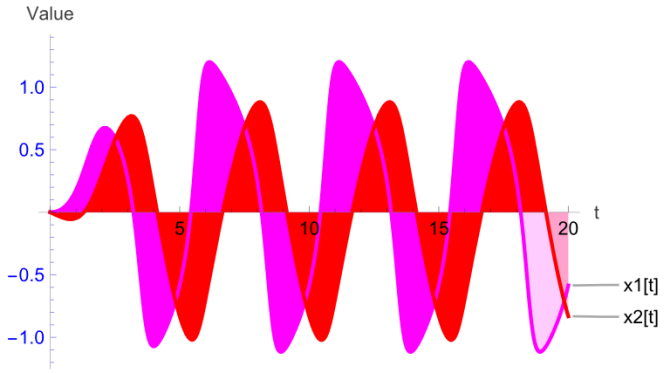
Case 1: electric activation rate parameter A=0.2



Case 2: electric activation rate parameter A=0.3



Case 3: electric activation rate parameter A=0.4



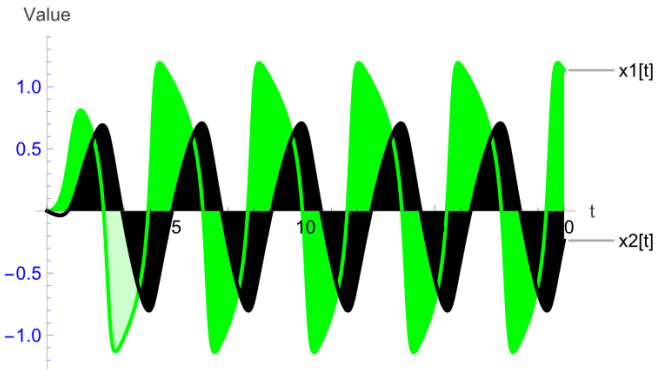
Case 4: electric activation rate parameter A=0.5

Fig. 9 Effect of variation in electric activation rate parameter on both state variables of heartbeat model by using Livermore solver for ordinary differential equation method

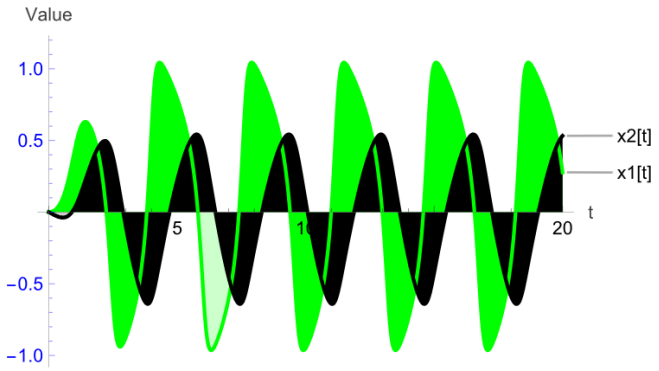
4.2 Problem 2: Effect of Muscle Fiber Tension B

In Problem 2, we study the effect of variation in the values of the parameter muscle fiber tension, i.e., B=1, 0.75, 0.5, and 0.25, while keeping fixed values of other parameters A=0.25 and F=0.1. the Muscle fiber tension parameter B impacts the amplitude and nonlinearity of HBM system.

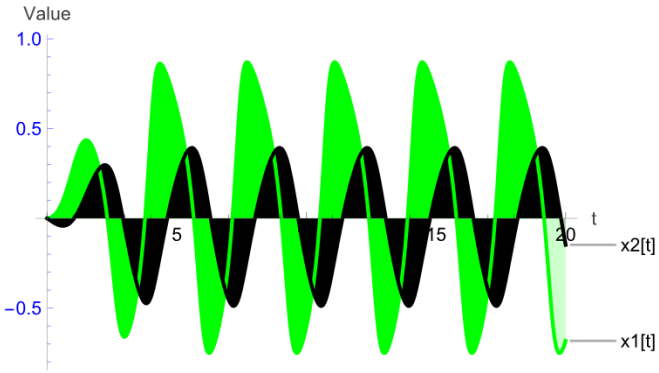
From the results, we see that decreasing the value of the muscle fiber tension parameter B leads to a substantial fall in the oscillation amplitude for both x1 and x2. For value B=1 the amplitude of x1 and x2 approach around values 1.2 and 0.7 respectively, for value B=0.75 the amplitudes of x1 and x2 are around 1 and 0.5, respectively, whereas for the value B=0.5 these values are 0.9 and 0.4, and finally for the value B=0.25 we get the values for x1 and x2 as 0.6 and 0.2 respectively which is a huge drop in the amplitude. Practically, we cannot decrease the value of parameter B below 0.2, as it will result in lower amplitude, and the heart would not be able to pump blood to the whole body, as it would not be able to generate a reasonable pressure. For all the 4 cases of problem 2, results produced by each proposed methodology are all nearly identical, which indicates stability and non-stiffness for these techniques. But, as we decrease the value of B, the nonlinearity becomes more pronounced.



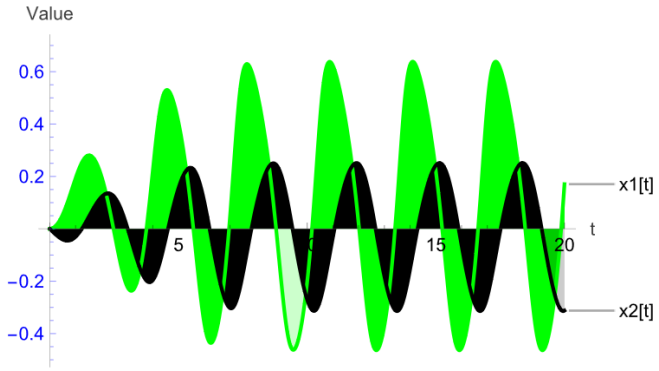
Case 1: muscle fiber tension parameter B=1



Case 2: muscle fiber tension parameter B=0.75



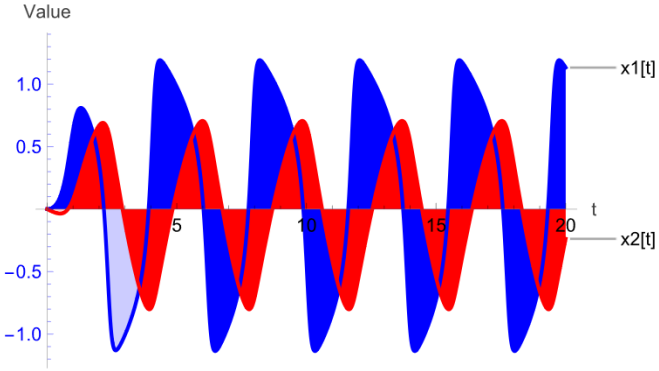
Case 3: muscle fiber tension parameter B=0.5



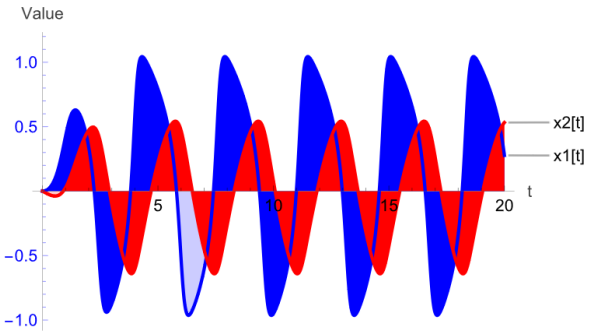
Case 4: muscle fiber tension parameter B=0.25

Fig. 10 Effect of variation in muscle fiber tension parameter B on both state variables of heartbeat model by using Adams predictor-corrector (APC) method

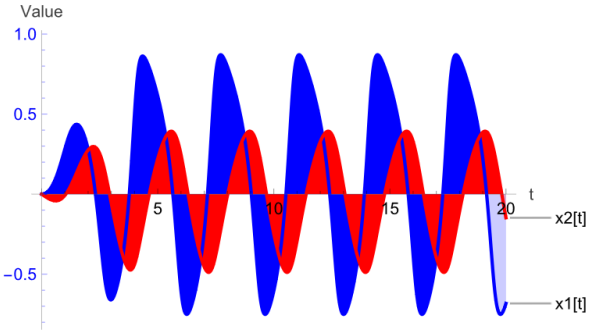
The Adam method is used as the reference method and the results for all the cases of problem 2 solved by the Adams APC method are presented in Figure 7, while the results for other methods BDS, AE-RK, AI-RK, SS and LSOD, are given in Figure 8, Figure 9, Figure 10, Figure 11, and Figure 12, respectively. The BDS method given in Figure 8 starts deviating from the reference APC results, specifically in obtaining peak amplitudes, as the values are slightly higher than the reference solution. The AE-RK given in Figure 9 follows the general trend but demonstrates minor smoothing of the sharp peaks. In contrast, AI-RK (Figure 10, SS (Figure 11, and LSOD (Figure 12 perfectly uphold both phase and amplitude, supporting their robustness and stability in handling the nonlinearity. Overall, the results gained from all the techniques imply that precise solution of peak dynamics needs stable and robust numerical methodologies.



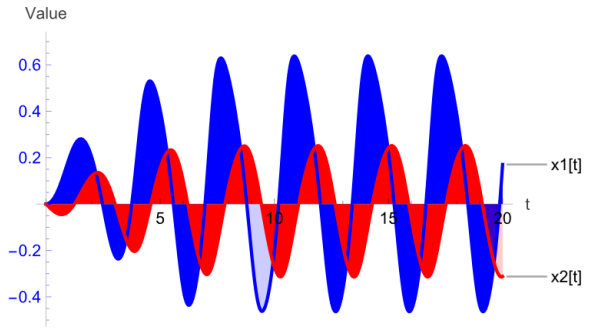
Case 1: muscle fiber tension parameter B=1



Case 2: muscle fiber tension parameter B=0.75

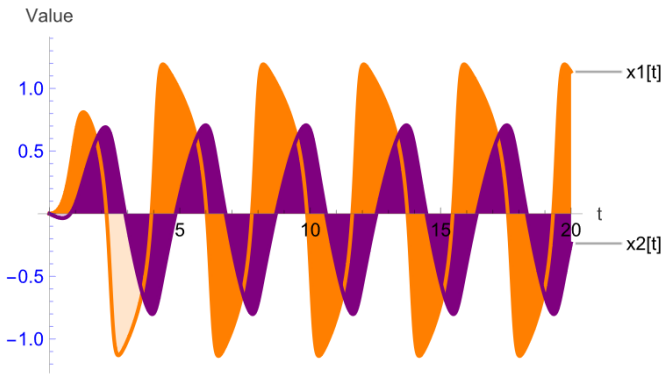


Case 3: muscle fiber tension parameter B=0.5

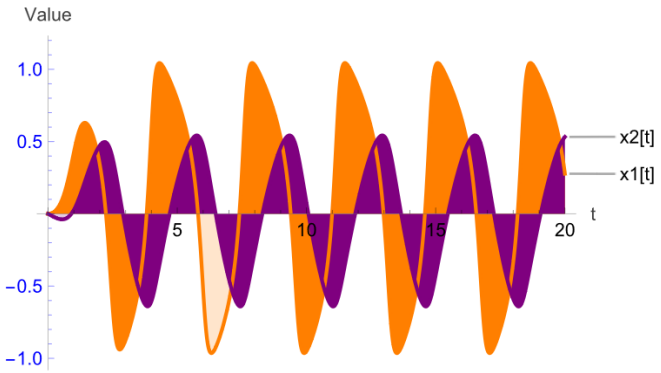


Case 4: muscle fiber tension parameter B=0.25

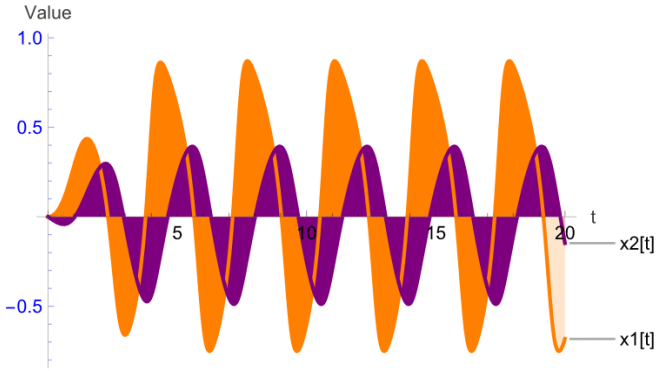
Fig. 11 Effect of variation in muscle fiber tension parameter B on both state variables of heartbeat model by using Backward difference formula



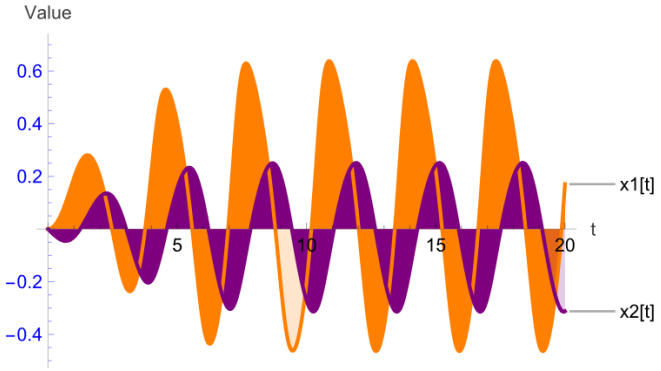
Case 1: muscle fiber tension parameter B=1



Case 2: muscle fiber tension parameter B=0.75

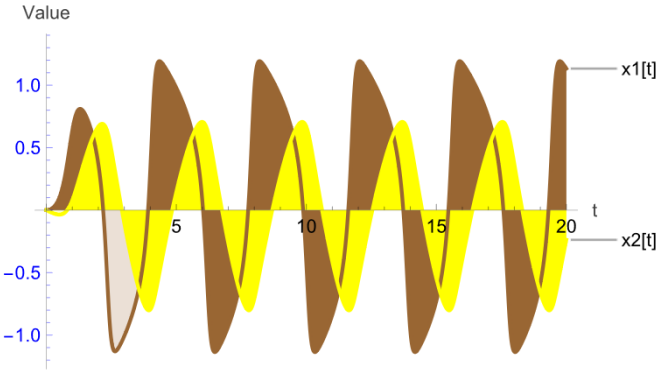


Case 3: muscle fiber tension parameter B=0.5

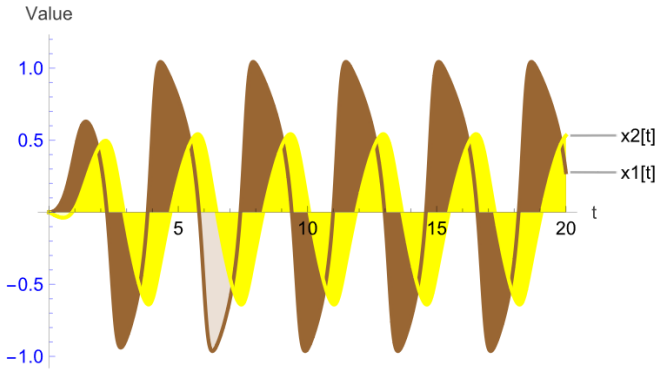


Case 4: muscle fiber tension parameter B=0.25

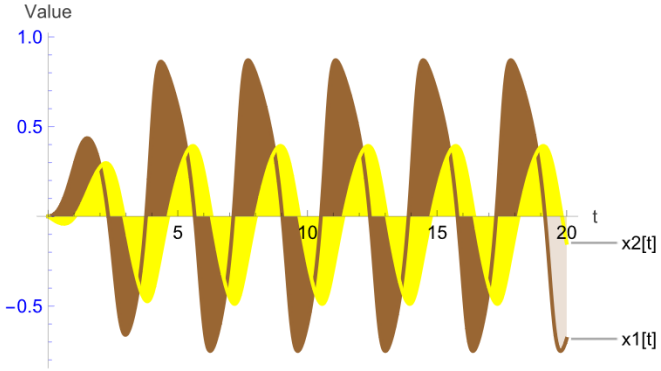
Fig. 12 Effect of variation in muscle fiber tension parameter B on both state variables of heartbeat model by using Explicit Range Kutta Method



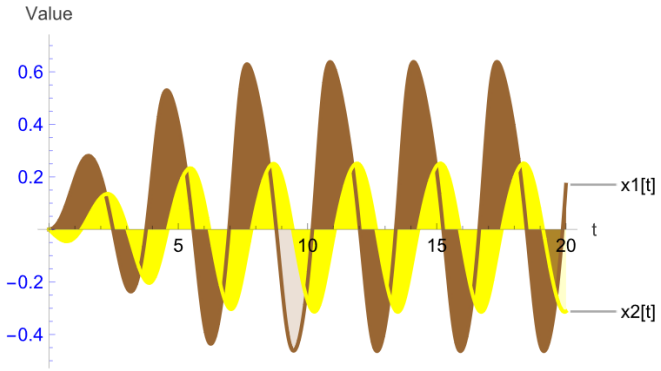
Case 1: muscle fiber tension parameter B=1



Case 2: muscle fiber tension parameter B=0.75

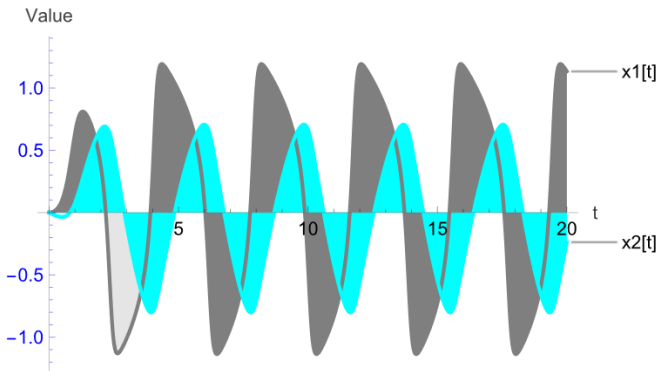


Case 3: muscle fiber tension parameter B=0.5

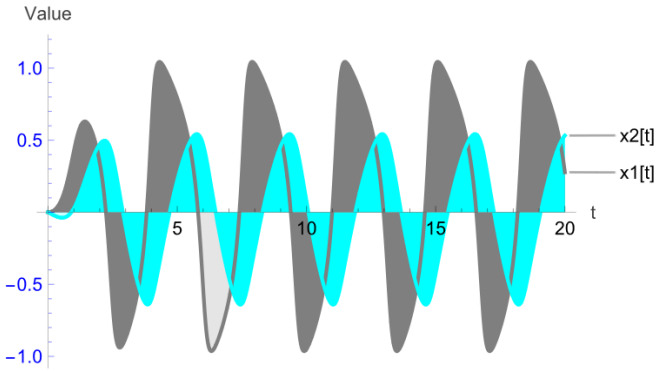


Case 4: muscle fiber tension parameter B=0.25

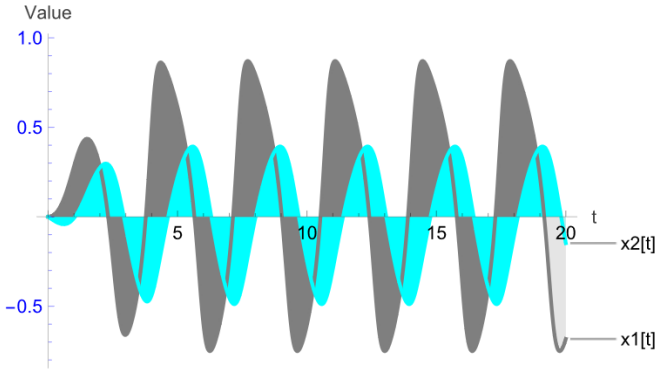
Fig. 13 Effect of variation in muscle fiber tension parameter B on both state variables of heartbeat model by using Implicit Range Kutta Method



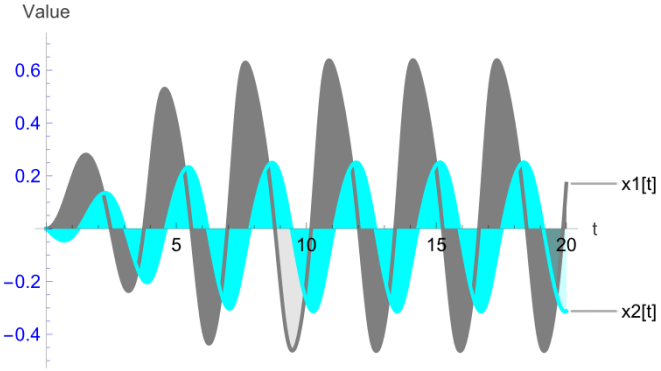
Case 1: muscle fiber tension parameter B=1



Case 2: muscle fiber tension parameter B=0.75

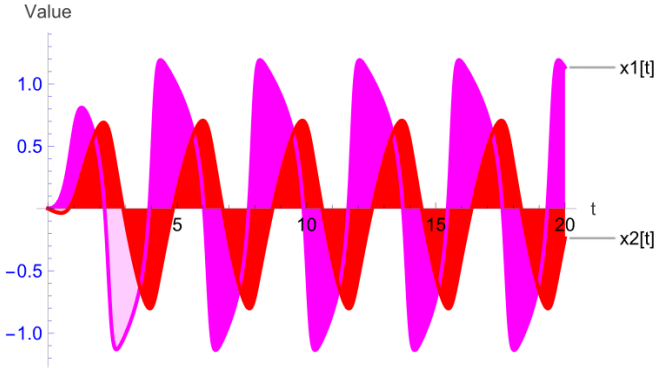


Case 3: muscle fiber tension parameter B=0.5

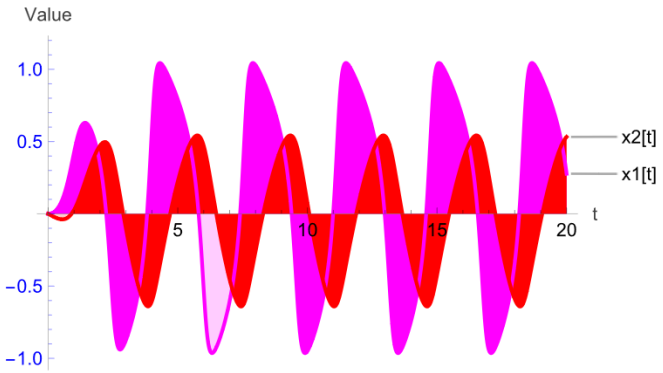


Case 4: muscle fiber tension parameter B=0.25

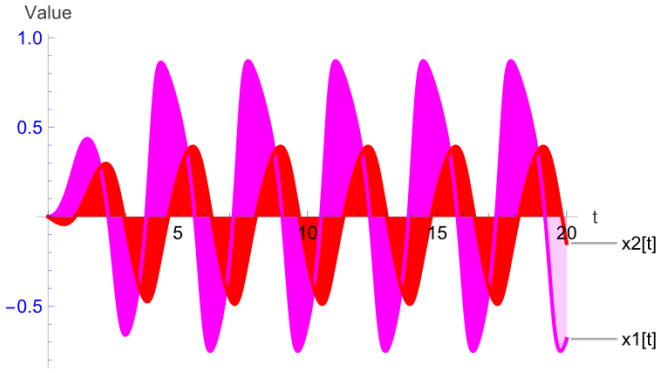
Fig. 14 Effect of variation in muscle fiber tension parameter B on both state variables of heartbeat model by using Stiffness switching Method



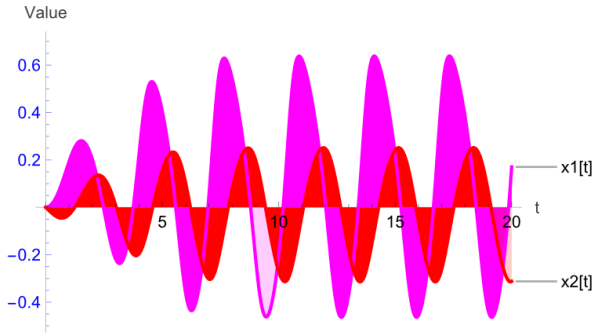
Case 1: muscle fiber tension parameter B=1



Case 2: muscle fiber tension parameter B=0.75



Case 3: muscle fiber tension parameter B=0.5



Case 4: muscle fiber tension parameter B=0.25

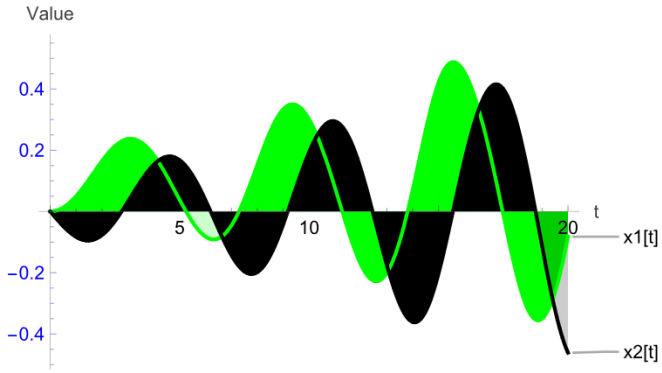
Fig. 15 Effect of variation in muscle fiber tension parameter B on both state variables of heartbeat model by using Livermore solver for ordinary differential equation method

4.3 Problem 3: Effect of Muscle Fiber Length F

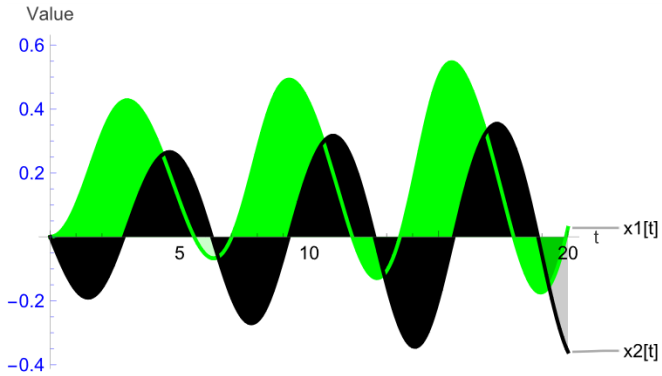
In this Problem, the 4 cases are formulated by varying the diastolic muscle fiber length F parameter, i.e., F=0.1, 0.2, 0.3, 0.4, while taking fixed values for A= 1and B=0.25 for each case. Unlike the eigenvalue parameter A and the muscle fiber tension parameter B, this parameter mainly affects the growth and decay in amplitude over time and phase characteristics.

It has been revealed from the numerical results that varying the F parameter shifts the equilibrium position of the HBM system, which results in a vertical shift in the waveform for both state variables x1 and x2. No change in the frequency of oscillations has been observed, but we noticed a small variation in phase and changes in waveform symmetry.

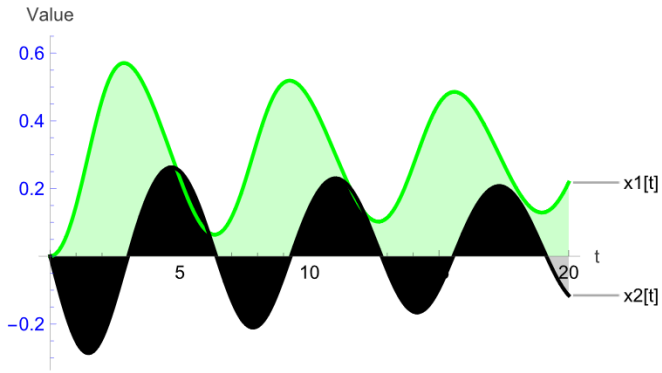
For the value F=0.1, we noticed an increasing trend in the amplitude value from 0.22 to 0.44 over the time period t=[0 20] for variable x1, whereas for x2, amplitude values increased from 0.2 to 0.4, slightly lower than x1, but we can clearly notice the phase shift in x1 and x2. For F=0.2, the same increasing pattern for amplitude was observed, but in this case the amplitude is not increasing so Fast; just a small increase in the amplitude was observed, with the same phase shift as in the previous case. In the third case, for the value of F=0.3, we observed a decreasing trend in the amplitude from the value around 0.6 to 0.2 for x1 and a slightly decreasing trend in x2.



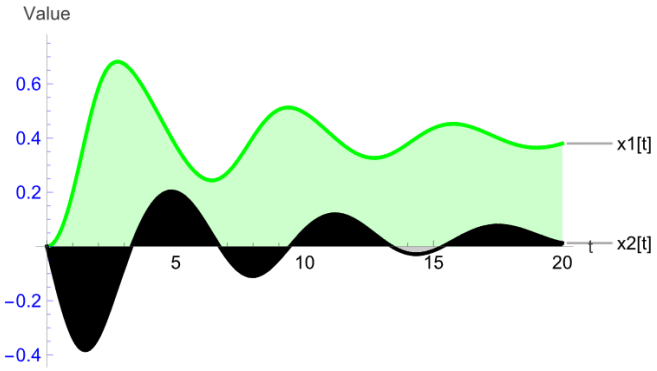
Case 1: muscle fiber length parameter F=0.1



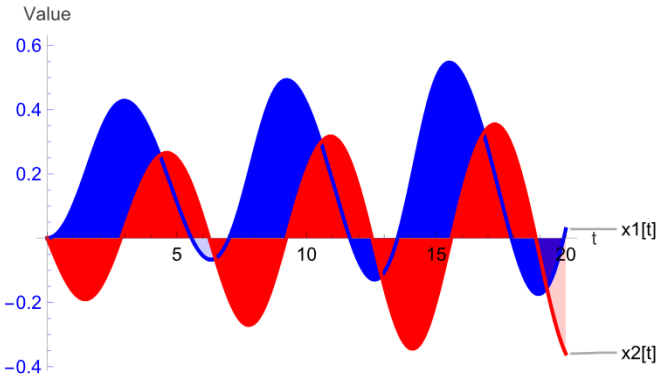
Case 2: muscle fiber length parameter F=0.2



Case 3: muscle fiber length parameter F=0.3



Case 4: muscle fiber length parameter F=0.4

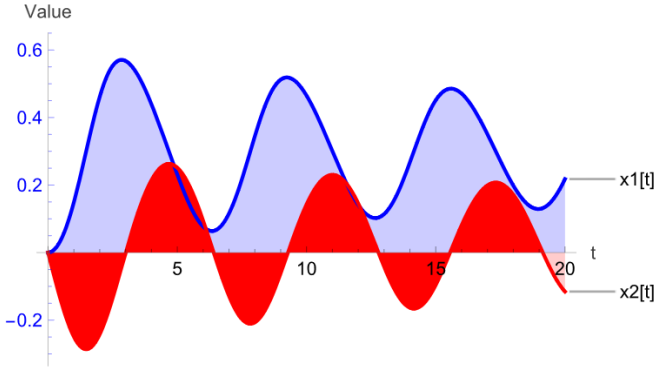


Case 2: muscle fiber length parameter F=0.2

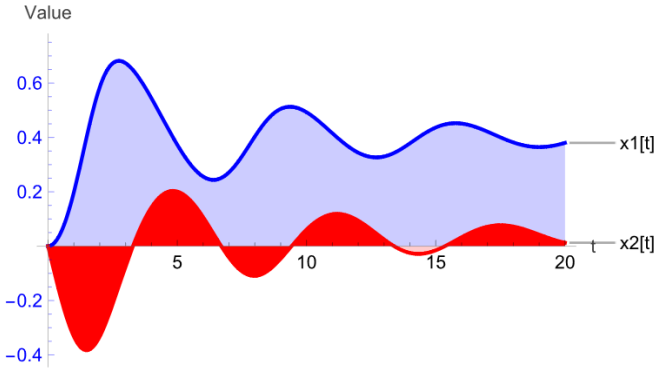
Fig. 16 Effect of variation in muscle fiber length parameter F on both state variables of heartbeat model by using Adams predictor-corrector (APC) method

Unlike the previous two cases, we observed a totally different trend in amplitude variation over the time period. In the last case, for F=0.4, we observed the same pattern as case 3, the amplitude is decreasing over the time period, but here the variation is too fast at the start the value of amplitude is higher than all the other cases, that is, around 0.64 for x1 but with the passage of time it tends towards zero, same is in the case of x2. Therefore, for the first two cases we observed an increasing trend, and for the last two cases we observed a decreasing trend; for the last case, we observed the worst pattern, as it is almost approaching zero. So, F=0.2 is the threshold value for the heart muscle length parameter.

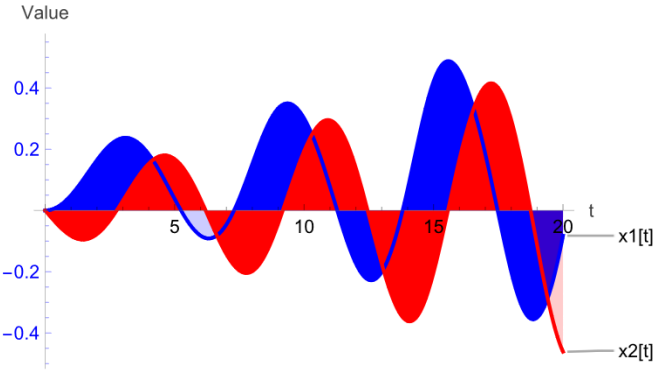
We have observed that all the proposed methodologies perform adequately for all the variations in heart fiber length parameter values. The results for all the proposed methodologies are given in Figures 13 to 18, with each case given as subplots. All the techniques steadily deliver accurate results, efficiently obtaining phase shifts and maintaining the structure of waveforms.



Case 3: muscle fiber length parameter F=0.3

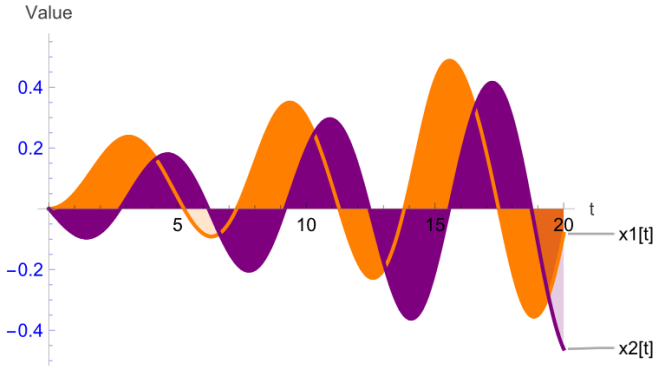


Case 4: muscle fiber length parameter F=0.4

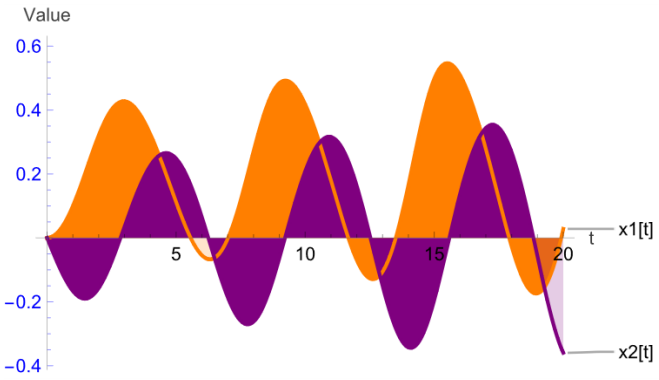


Case 1: muscle fiber length parameter F=0.1

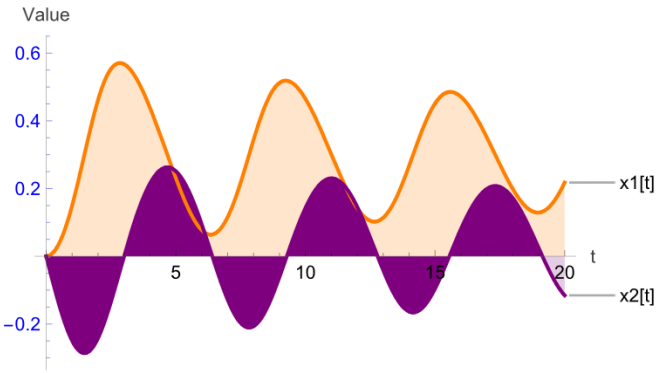
Fig. 17 Effect of variation in muscle fiber length parameter F on both state variables of heartbeat model by using backward difference formula



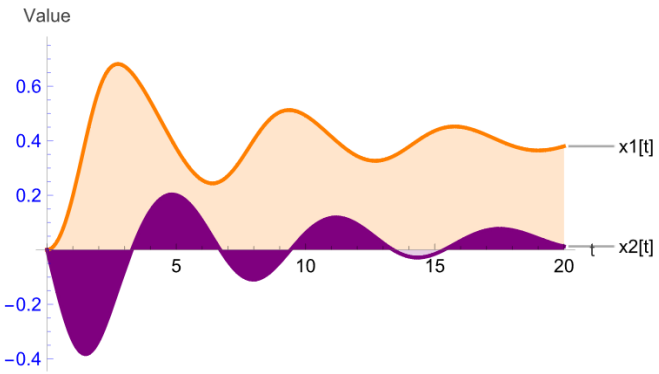
Case 1: muscle fiber length parameter F=0.1



Case 2: muscle fiber length parameter F=0.2

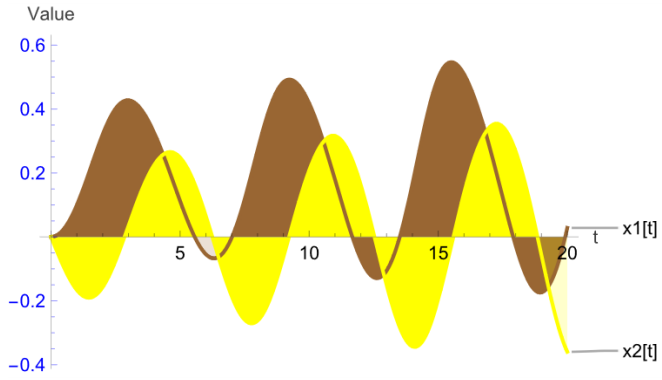


Case 3: muscle fiber length parameter F=0.3

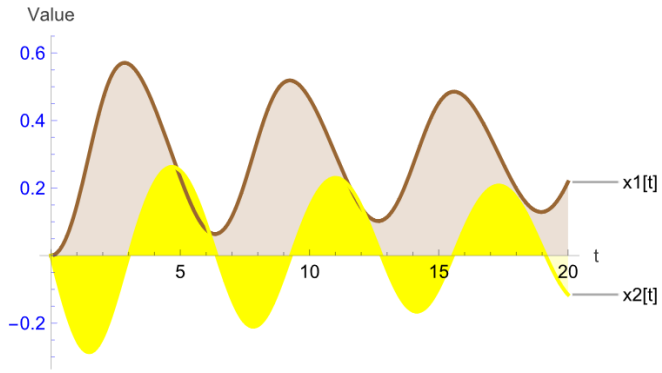


Case 4: muscle fiber length parameter F=0.4

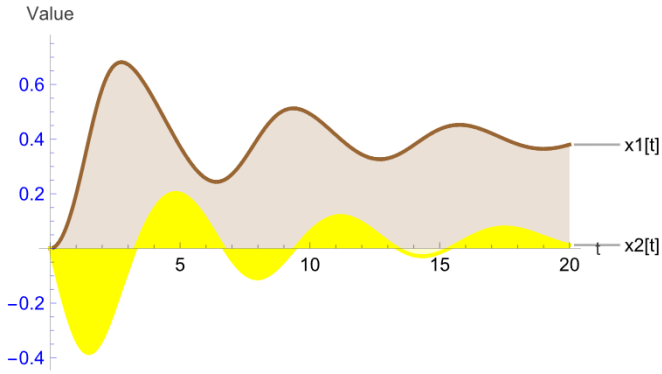
Fig. 18 Effect of variation in muscle fiber length parameter F on both state variables of heartbeat model by using Explicit Range Kutta Method



Case 2: muscle fiber length parameter F=0.2

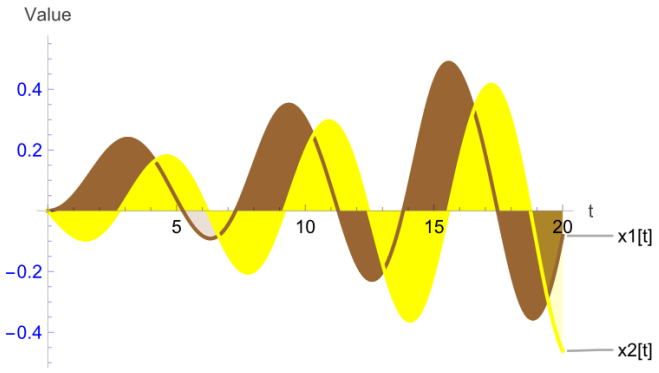


Case 3: muscle fiber length parameter F=0.3

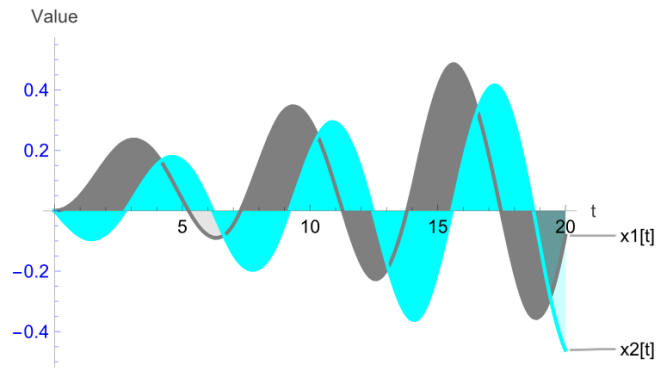


Case 4: muscle fiber length parameter F=0.4

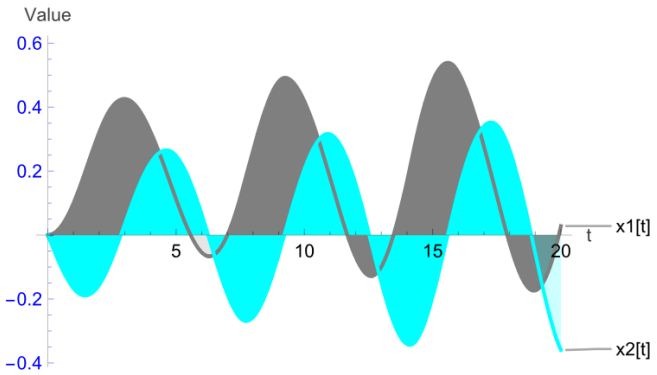
Fig. 19 Effect of variation in muscle fiber length parameter F on both state variables of heartbeat model by using Implicit Range Kutta Method



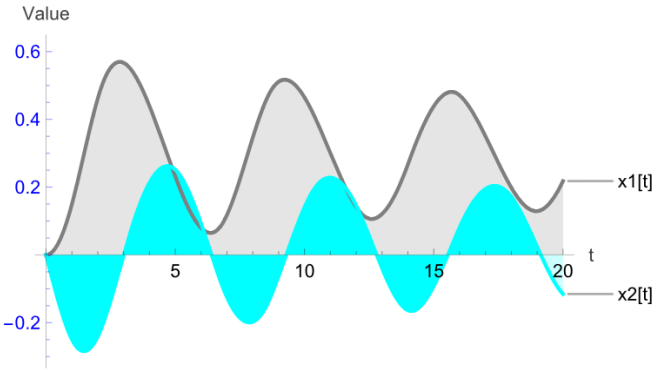
Case 1: muscle fiber length parameter F=0.1



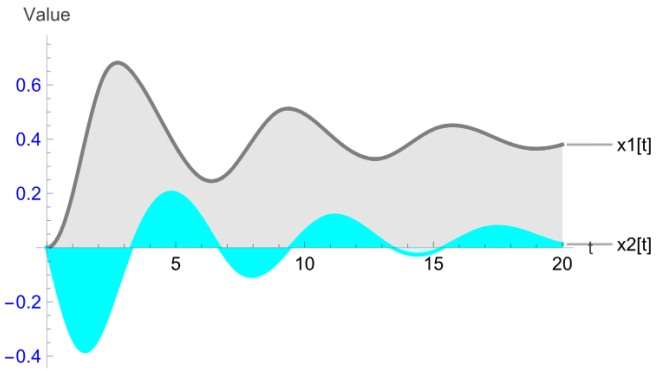
Case 1: muscle fiber length parameter F=0.1



Case 2: muscle fiber length parameter F=0.2

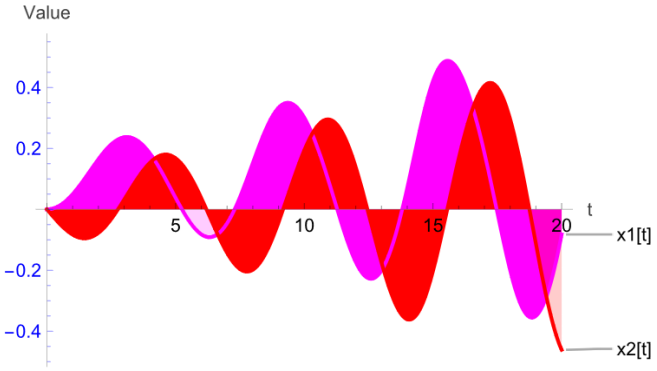


Case 3: muscle fiber length parameter F=0.3

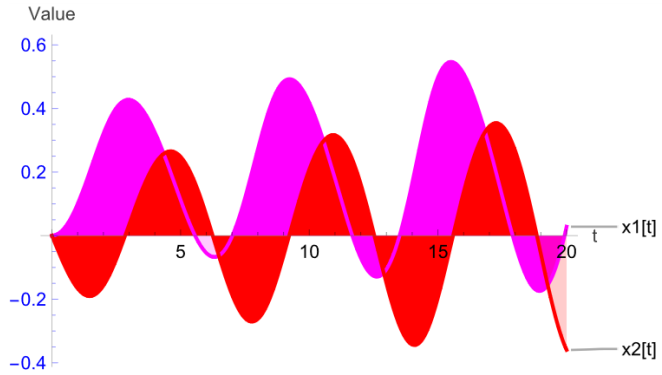


Case 4: muscle fiber length parameter F=0.4

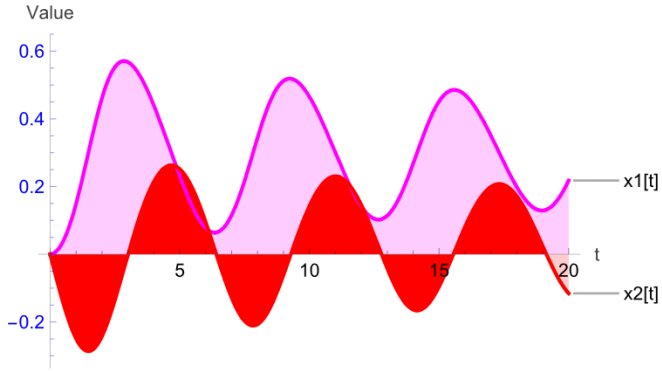
Fig. 20 Effect of variation in muscle fiber length parameter F on both state variables of heartbeat model by using Stiffness switching Method



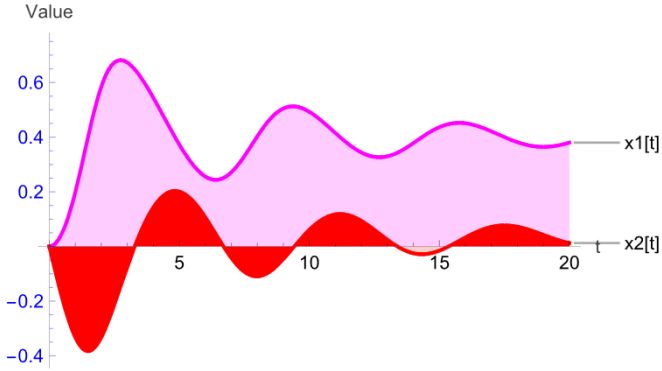
Case 1: muscle fiber length parameter F=0.1



Case 2: muscle fiber length parameter F=0.2



Case 3: muscle fiber length parameter F=0.3



Case 4: muscle fiber length parameter F=0.4

Fig. 21 Effect of variation in muscle fiber length parameter F on both state variables of heartbeat model by using Livermore solver for ordinary differential equation Method

4.4 Compara ve Analysis

From the comparative analysis, it has been seen that the trend is uniform for all the proposed methodologies for each problem. In problems 1 and 2, for higher values of parameters A and B, as nonlinearity and stiffness increase, the implicit technique AE-RK reveals slightly lower stability and accuracy. While AI-RK and adaptive techniques, including SS and LSOD, sustain high accuracy in all cases.

It has been observed that the variation in amplitude is mostly affected by the variation in the values of B, while the frequency is controlled by the variation in parameter A, and the angle shift and

growth and decay response of the system is affected by variation in F, for both the state variables x1 and x2.

4.5 Error and Performance Evaluation

The quantitative assessment for all the cases of each problem was carried out using Mean Absolute Error (MAE), Mean Absolute Deviation (MAD), Nash–Sutcliffe Efficiency (NSE), and Thiel's Inequality Coefficient (TIC), and the results are presented in Table 1 given below. Also, the Absolute Error (AE) plots for problems 1, 2, and 3 are given in Figure 22, Figure 23, and Figure 24, respectively, for the Explicit Runge Kutta method with the reference Adams method.

Table 1 Statistical performance indices for all 3 problems of HBM

Problems	Cases	parameters	MAE	MAD	NSE	TIC
Problem 1	Case1	x_1	6.27775E-5	8.19917E-5	1	1.2617E-4
		x_2	5.23233E-6	6.23912E-6	1	1.69253E-5
	Case 2	x_1	6.46E-5	7.84E-05	1	0.00012
		x_2	7.67522E-6	8.95534E-6	1	2.14E-05
	Case 3	x_1	6.67E-05	7.98E-05	1	0.000136215
		x_2	9.45E-06	1.03E-05	1	2.19738E-05
	Case 4	x_1	5.77E-05	6.44E-05	1	9.98057E-05
		x_2	9.39E-06	9.72E-06	1	1.82581E-05
Problem 2	Case 1	x_1	5.89E-05	7.22E-05	1	0.000104625
		x_2	6.67E-06	7.96E-06	1	1.94885E-05
	Case 2	x_1	5.66E-05	6.61E-05	1	1.22E-04
		x_2	6.31E-06	6.68E-06	1	2.06754E-05
	Case 3	x_1	6.42E-05	7.01E-05	1	0.00015882
		x_2	8.13E-06	7.96E-06	1	3.51723E-05
	Case 4	x_1	5.65E-05	5.75E-05	1	0.000204836
		x_2	9.77E-06	1.01E-05	1	6.74165E-05
Problem 3	Case 1	x_1	5.47E-05	5.81E-05	1	0.000179257
		x_2	4.66E-06	4.44E-06	1	0.000046131
	Case 2	x_1	4.05E-05	4.38E-05	1	0.000143502
		x_2	4.26E-06	4.61E-06	1	0.000051102
	Case 3	x_1	1.42E-05	1.52E-05	1	6.56168E-05
		x_2	3.65E-06	2.90E-06	1	7.42869E-05
	Case 4	x_2	1.11E-06	1.70E-06	1	7.38E-06
		x_2	2.25E-07	3.30E-07	1	0.00001175

The results indicate that LSOD and IRK methods achieve the lowest maximum error across all problems. Stiffness Switching also performs competitively, particularly in adaptive scenarios. The MAD values for these methods remain minimal, while NSE values are consistently close to unity, indicating excellent agreement with the reference solution. Furthermore, Thiel's inequality coefficient remains close to zero, confirming the reliability of these methods.

In contrast, ERK and Adams methods exhibit increasing error with higher stiffness and nonlinearity, particularly in Problems 1 and 2.

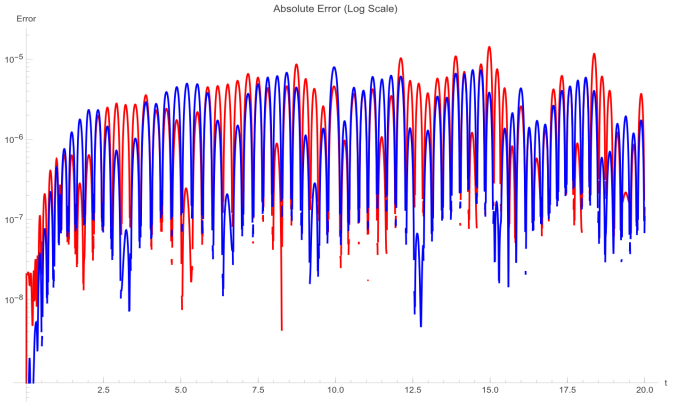


Fig. 22 Absolute error plot for Explicit range Kutta method with reference Adams Method for problem 1

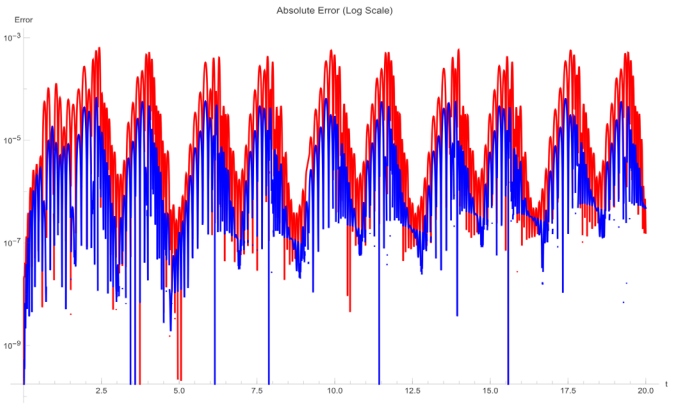


Fig. 23 Absolute error plot for Explicit range Kutta method with reference Adams Method for problem 2

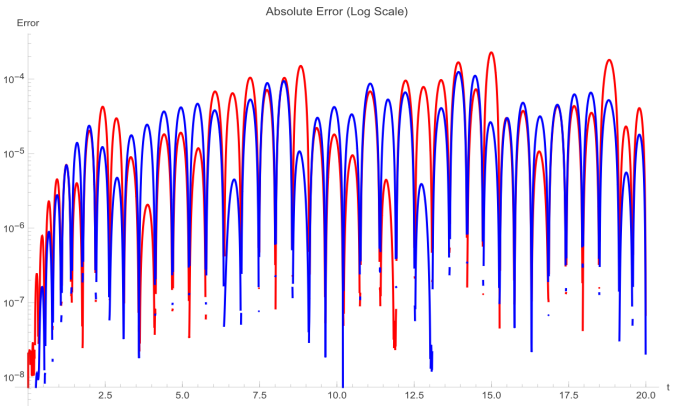


Fig. 24 Absolute error plot for Explicit range Kutta method with reference Adams Method for problem 3

The complexity analysis for all the proposed methodologies for each problem have been done based on time taken, function evaluation, step count, maximum error and memory used by each methodology and from the results one may observed that BDS method takes more memory, time taken to evaluate the solution and step counts while less maximum error as compared to other proposed techniques which makes it more complex but accurate than the rest of proposed methodologies.

4.6 Discussion

The results clearly demonstrate that the choice of numerical method plays a crucial role in accurately simulating the heartbeat model. While Adams and ERK methods are suitable for mildly stiff or non-stiff systems, they become less reliable as stiffness and nonlinearity increase. On the other hand, IRK, LSOD, and Stiffness Switching methods provide superior performance in terms of accuracy, stability, and robustness.

The structured parametric analysis, combined with detailed graphical interpretation, provides comprehensive insight into the dynamic behavior of the HBM. The consistency between graphical observations and quantitative metrics further validates the effectiveness of the proposed numerical framework.

Overall, the study highlights the importance of adaptive and stiff-aware numerical techniques for solving complex physiological models and establishes a reliable approach for analyzing heartbeat dynamics under varying parametric conditions.

5. CONCLUSION

In this study, a comprehensive numerical examination of the nonlinear heartbeat model (HBM) was done by using different numerical methods, which include the Adams predictor-corrector method, the explicit Runge- Kutta method, the implicit Runge–Kutta method, the stiffness-switching method, and the LSOD method. Here, the solution of the Adams predictor-corrector method was used as a reference, and the performance of the rest of the techniques was assessed via stability, accuracy, and computational complexity analysis.

The results shows that all proposed techniques reproduce the subjective oscillatory behavior of the heartbeat model over the time interval t = [0, 20]. Conversely, substantial variations occur in computational efficiency and accuracy, especially under variable levels of nonlinearity and stiffness. The explicit Runge-Kutta method performs reasonably well for stiff cases but shows instability and amplitude changes as stiffness increases. Likewise, the implicit Runge- Kutta method, though used as a reference, shows weaknesses in highly stiff routines.

On the other hand, LSOD, Stiffness Switching, and BDS method always provide better stability and accuracy across all cases. These techniques successfully manage nonlinearities and stiffness, preserving near agreement with the Adam reference solution while decreasing the error.

The parametric analysis, structured into three problems, provides deeper insight into the influence of key model parameters. Variation in the electric activation of heart parameter (A) primarily affects system stiffness and oscillation frequency, variation in the tension parameter (B) controls amplitude and peak sharpness, and variation in the fiber length (F) influences baseline and phase characteristics. The graphical analysis confirms that increasing stiffness and nonlinearity significantly impact the performance of numerical solvers, emphasizing the importance of appropriate method selection.

Furthermore, the evaluation based on performance indices, including mean absolute deviation (MAD), Nash–Sutcliffe efficiency (NSE), and Thiel's inequality coefficient, validates the reliability and effectiveness of the proposed numerical framework. LSOD and Stiffness Switching methods, in particular, achieve the best balance between accuracy and computational efficiency.

In conclusion, the study establishes that adaptive and stiff-aware numerical methods are essential for accurately solving

complex physiological models such as the heartbeat model. The proposed approach, combining multiple numerical techniques with systematic parametric analysis, provides a robust and reliable framework for investigating nonlinear dynamical systems in biomedical applications. Future work may focus on extending the model to incorporate additional physiological factors and exploring real-time simulation capabilities for clinical applications.

REFERENCES

[1] Vigmond, E., Vadakkumpadan, F., Gurev, V., Arevalo, H., Deo, M., Plank, G. and Trayanova, N., 2009. "Towards predictive modelling of the electrophysiology of the heart." *Experimental physiology,* **94**(5), pp.563-577.

[2] Labarthe, D.R., Dai, S., Day, R.S., Fulton, J.E., Grunbaum, J.A., Shah, S.M. and Wen, E., 2009. "Project HeartBeat!: concept, development, and design." *American journal of preventive medicine,* **37**(1), pp.S9-S16.

[3] Al-Salimi, B.H.S., 2009. *Mathematical modeling of the heartbeat.* Sultan Qaboos University (Oman).

[4] Danilov, V., Litvinov, R. and Gerget, O., 2016, "May. Mathematical modeling the electrical activity of the heart." *In Information Technologies in Science, Management, Social Sphere and Medicine* (pp. 361-365). Atlantis Press.

[5] Kuhtz-Buschbeck, J.P., Schaefer, J., Wilder, N. and Wolze, W.T., 2021. "The origin of the heartbeat and theories of muscle contraction. Physiological concepts and conflicts in the 19th century." *Progress in Biophysics and Molecular Biology,* **159**, pp.3-9.

[6] Niederer, S.A., Lumens, J. and Trayanova, N.A., 2019. "Computational models in cardiology." *Nature reviews cardiology,* **16**(2), pp.100-111.

[7] Signorini, M.G. and Di Bernardo, D., 1998. "Simulation of heartbeat dynamics: a nonlinear model." *International journal of Bifurcation and Chaos,* **8**(08), pp.1725-1731.

[8] Thanom, W. and Loh, R.N.K., 2011. "Nonlinear control of heartbeat models." *Journal on systemics, Cybernetics and Informatics,* **9**(1), pp.21-27.

[9] Danilov, V., Litvinov, R. and Gerget, O., 2016, "May. Mathematical modeling the electrical activity of the heart." *In Information Technologies in Science, Management, Social Sphere and Medicin*e (pp. 361-365). Atlantis Press.

[10] Signorini, M.G. and Di Bernardo, D., 1998. "Simulation of heartbeat dynamics: a nonlinear model." *International journal of Bifurcation and Chaos,* **8**(08), pp.1725-1731.

[11] Kalyan, V., 2024. "Transverse Tubules in Cardiac Health and Disease: Therapeutic Approaches to T-Tubule Remodelling and Heart Failure Management." *International Journal of Drug Discovery and Pharmacology,* **3**(4), p.100024.

[12] Izhikevich, E.M. and FitzHugh, R., 2006. "Fitzhugh-nagumo model." *Scholarpedia,* **1**(9), p.1349.

[13] Cveticanin, L., 2013. "On the Van der Pol oscillator: An overview." *Applied Mechanics and Materials,* **430**, pp.3-13.

[14] Tuinenburg, J.C., Koning, G., Rareş, A., Janssen, J.P., Lansky, A.J. and Reiber, J.H., 2011. "Dedicated bifurcation analysis: basic principles." *The International Journal of Cardiovascular Imaging,* **27**(2), pp.167-174.

[15] Huang, B.F. and Boutros, P.C., 2016. "The parameter sensitivity of random forests." *BMC bioinformatics,* **17**(1), p.331.

[16] Huang, B.F. and Boutros, P.C., 2016. "The parameter sensitivity of random forests." *BMC bioinformatics,* **17**(1), p.331.

[17] Quintana, D.S., 2017. "Statistical considerations for reporting and planning heart rate variability case-control studies." *Psychophysiology,* **54**(3), pp.344-349.

[18] Balamurugan, M. and Meera, S., 2026. "An Intellectual Framework for Heart Disease Detection Using Multi-Scale Convolutional Autoencoder With Adaptive Gated Recurrent Unit." *International Journal of Adaptive Control and Signal Processing.*

[19] Pozo, M.R., Pressler, M.P., Horvath, A. and Entcheva, E., 2026. "Comparative transcriptomics analysis of histone deacetylases, transcription factors, and ion channel genes in human iPSC-cardiomyocytes vs. the adult human heart." *bioRxiv,* pp.2026-01.

[20] Karmelic, D., Steinberg, Y., Jones, R.T., Genç, Ö. and Davis, G.W., 2026. "Homeostatic preservation of action potential waveform by Notch and Nerfin-1." *Current Biology,* **36**(5), pp.1166-1179.

[21] Ahmad, Z., Yin, M., Sukurdeep, Y., Rotenberg, N., Kholmovski, E. and Trayanova, N.A., 2024. "Elastic shape analysis computations for clustering left atrial appendage geometries of atrial fibrillation patients." *Arxiv*, pp.arXiv-2403.

[22] Win, K.Z., Armstrong, M.J., Steeds, R.P. and Kalla, M., 2025. Clinical Electrophysiology and Ablation.

[23] Chen, X., Zhang, K., Ji, Z., Shen, X., Liu, P., Zhang, L., Wang, J. and Yao, J., 2023. "Progress and challenges of integrated machine learning and traditional numerical algorithms: Taking reservoir numerical simulation as an example." *Mathematics,* **11**(21), p.4418.

[24] Lu, Y., Zhang, H., Xu, D. and Huang, W.X., 2025. "Nonlinear tunable stiffness for high-efficiency biomimetic propulsion." *Journal of Fluid Mechanics,* **1017**, p.A7.

[25] Feischl, M. and Niederkofler, D., 2025. "Optimal adaptive implicit time stepping." *arXiv preprint* arXiv:2506.18809.

[26] Soares Jr, D., 2025. "An adaptive time integration procedure for automated extended-explicit/implicit hybrid analyses." *Engineering with Computers,* **41**(1), pp.535-564.

[27] Zaky, M.A., 2025. "Finite difference/fractional pertrov–galerkin spectral method for linear time-space fractional reaction–diffusion equation." *Mathematics,* **13**(11), p.1864.

[28] Wei, S., Guenter, V. and Spiteri, R.J., 2025. "Improving the Stability and Efficiency of Operator-Splitting Methods." *SIAM Journal on Scientific Computing,* **47**(3), pp.A1888-A1906.

[29] Morotti, S., 2025. "Precision cardiac electrophysiology: Toward digital twins and beyond." *The Journal of Precision Medicine: Health and Disease, 2.*

[30] Centofanti, E., Ziarelli, G., Scacchi, S. and Pavarino, L.F., 2026. "A Neural Latent Dynamics Approach for Solving Inverse Problems in Cardiac Electrophysiology." *arXiv preprint arXiv:2605.01463.*

[31] Pathmanathan, P., Aycock, K., Badal, A., Bighamian, R., Bodner, J., Craven, B.A. and Niederer, S., 2024. "Credibility as-

sessment of in silico clinical trials for medical devices." *PLoS computational biology,* **20**(8), p.e1012289.

[32] Dössel, O. and Loewe, A., 2025. "Computerized Modeling of Electrophysiology and Pathoelectrophysiology of the Atria--How Much Detail is Needed?." *arXiv preprint arXiv:2505.23717.*

[33] Clarivate, 2026. Web of Science Core Collection. Available at: https://www.webofscience.com (Accessed: 14 June 2026).

[34] Raja, M.A.Z., Shah, F.H., Alaidarous, E.S. and Syam, M.I., 2017. "Design of bio-inspired heuristic technique integrated with interior-point algorithm to analyze the dynamics of heartbeat model." *Applied Soft Computing,* **52**, pp.605-629.